

# Automated Ski Velocity and Jump Length Determination in Ski Jumping Based on Unobtrusive and Wearable Sensors

BENJAMIN H. GROH, Friedrich-Alexander-Universität Erlangen-Nürnberg (FAU)  
 FRANK WARSCHUN, Institute for Applied Training Science Leipzig (IAT)  
 MARTIN DEININGER, Otto-von-Guericke-Universität Magdeburg (OvGU), Germany  
 THOMAS KAUTZ, Friedrich-Alexander-Universität Erlangen-Nürnberg (FAU)  
 CHRISTINE MARTINDALE, Friedrich-Alexander-Universität Erlangen-Nürnberg (FAU)  
 BJOERN M. ESKOFIER, Friedrich-Alexander-Universität Erlangen-Nürnberg (FAU)

---

Although ski jumping is a widely investigated sport, competitions and training sessions are rarely supported by state-of-the-art technology. Supporting technologies could focus on a continuous velocity determination and visualization for competitions as well as on an analysis of the velocity development and the jump length for training sessions. In the literature, there are several approaches for jump analysis. However, the majority of these approaches aim for a biomechanical analysis instead of a support system for frequent use. They do not fulfill the requirements of unobtrusiveness and usability that are necessary for a long-term application in competitions and training. In this paper, we propose an algorithm for ski velocity calculation and jump length determination based on the processing of unobtrusively obtained ski jumping data. Our algorithm is evaluated with data from eleven athletes in two different acquisitions. The results show an error of the velocity measurement at take-off of  $-0.78 \frac{m}{s} \pm 1.18 \frac{m}{s}$  (which equals  $-3.0\% \pm 4.7\%$  in reference to the estimated average take-off velocity) compared to a light barrier system. The error of the jump length compared to a video-based system is  $0.8 \text{ m} \pm 2.9 \text{ m}$  (which equals  $0.9\% \pm 3.4\%$  of the average jump length of the training jumps in this work). Although our proposed system does not outperform existing camera-based methods of jump length measurements at competitions, it provides an affordable and unobtrusive support for competitions and has the potential to simplify analyses in standard training.

**CCS Concepts:** • **Information systems** → **Data analytics**; • **Human-centered computing** → **Ubiquitous and mobile computing systems and tools**;

**Additional Key Words and Phrases:** Data processing, Wearable sensors, Sports, Ski jumping

**ACM Reference Format:**

Benjamin H. Groh, Frank Warschun, Martin Deininger, Thomas Kautz, Christine Martindale, and Bjoern M. Eskofier. 2017. Automated Ski Velocity and Jump Length Determination in Ski Jumping Based on Unobtrusive and Wearable Sensors. *Proc. ACM Interact. Mob. Wearable Ubiquitous Technol.* 1, 3, Article 53 (September 2017), 17 pages.  
 DOI: <http://doi.org/10.1145/3130918>

---

Author's addresses: B. H. Groh and T. Kautz and C. Martindale and B. M. Eskofier, Digital Sports Group, Pattern Recognition Lab, Department of Computer Science, Friedrich-Alexander-Universität Erlangen-Nürnberg (FAU), Erlangen, Germany; F. Warschun, Institute for Applied Training Science Leipzig (IAT), Leipzig, Germany; M. Deininger, Institute of Sport Science (ISPW), Otto-von-Guericke-Universität Magdeburg (OvGU), Magdeburg, Germany

Contact author: B. H. Groh, [benjamin.groh@fau.de](mailto:benjamin.groh@fau.de).

Permission to make digital or hard copies of all or part of this work for personal or classroom use is granted without fee provided that copies are not made or distributed for profit or commercial advantage and that copies bear this notice and the full citation on the first page. Copyrights for components of this work owned by others than ACM must be honored. Abstracting with credit is permitted. To copy otherwise, or republish, to post on servers or to redistribute to lists, requires prior specific permission and/or a fee. Request permissions from [permissions@acm.org](mailto:permissions@acm.org).

© 2017 Association for Computing Machinery.

2474-9567/2017/9-ART53 \$15.00

DOI: <http://doi.org/10.1145/3130918>

## 1 INTRODUCTION

Ski jumping has a long history and was part of the first Winter Olympic Games held in 1924. Since then, extensive research has been published on ski jumping biomechanics [36, 37] and the improvement of jumping techniques [24, 30, 38, 39]. In contrast, state-of-the-art technology is rarely used to directly support competitions and training sessions. In competitions, the official jump length is obtained with camera-based measurements [23]. However, the availability of more jump parameters, such as a continuous ski velocity, would not only support judges in their decisions but also provide spectators with a deeper insight into the sport. In addition, training sessions are often analyzed based on simple video recordings which cover only parts of the jump, allowing only qualitative jump analysis. Information about the continuous ski velocity as well as the jump length is not available during standard training, although they could provide meaningful feedback for coaches and athletes. Hence, a system which provides the continuous velocity and jump length without the necessity of a complex camera-setup would lead to more interesting information at competitions and could improve the training of the athletes.

The application of such a system in competitions and training must meet several requirements. First, it should measure unobtrusively. The athletes are highly focused and should not be distracted by the measurement setup. Second, the system must work automatically, without the requirement of constant maintenance, which would not be feasible during competitions or even training scenarios. Third, the application in ski jumping training requires an affordable system that does not contain any complex or time-consuming setup.

A system based on wearable inertial-magnetic measurement units (IMMUs) could meet these requirements. IMMU devices are small, light-weight and can easily be attached to skis without any interaction from the athlete. Furthermore, a continuous data stream of acceleration, angular velocity and magnetometer data in combination with smart processing algorithms can lead to a maintenance-free automated system, which only requires human interaction for preparation tasks such as charging, calibration and attachment to the skis. Although such a system would not require external sensor hardware aside from the IMMU, it could be enhanced by external input such as light barriers, which are often already available at jumping hills. Acquired jump data can then be processed to provide a visualization of relevant jump parameters. These parameters could contain the ski orientation, continuous horizontal and vertical velocity, flight path and altitude or a combination of these components.

In the literature, several publications addressed the application of wearables in ski jumping. Chardonnens and colleagues intensively investigated the field of biomechanical analysis based on inertial sensors. In [12], they attached sensors to both the body and skis and determined several jump phases (e.g., inrun, take-off, flight phases) by fusing the information of all sensors. In [9], they determined body segment orientations and force parameters of the stable flight phase and compared them to literature values and jump performance. In a follow-up work, they analyzed the entire jump and incorporated biomechanical constraints in order to improve their method [10]. Chardonnens and colleagues additionally investigated a partially functional calibration in order to correct the influence of misaligned sensor attachment. They also proposed a dynamical analysis of the take-off. This analysis contained, amongst others, the athlete's acceleration, velocity and applied forces during take-off [11]. A similar study was conducted by Bächlin and colleagues [2] who analyzed the applied forces during jumps and the flight time based on acceleration sensors. Furthermore, Logar and Munih [28] estimated the jump kinematics and dynamics in order to calculate the ground reaction force during inrun and take-off. Brock et al. [7] estimated the orientation of several body segments and relative joint positions with nine inertial-magnetic sensors attached to the athlete's body. They furthermore stated in [8] that these kinematic parameters could be processed to an automated jump scoring. In previous work from our group [20], we proposed a simplified approach for an orientation determination of the skis. Jump angles were calculated with a method similar to the one of [10] but were additionally evaluated with a 2D-camera system. In the same publication, we described a functional calibration method without any required action from the athlete.

In summary, different approaches were proposed for the calculation of jump parameters (e.g., forces, acceleration, velocity, body orientation). However, most of these approaches aimed for a biomechanical analysis rather than providing direct support to competitions and training. These approaches neither contained a continuous ski velocity calculation for the flight phase nor a jump length determination based on wearable sensors. Furthermore, the majority of the proposed methods did not focus on unobtrusiveness but rather based their work on sensors attached to the athletes' bodies. While such an attachment is required for extensive biomechanical analysis, it is not feasible for competitions and hardly applicable to standard training sessions.

In this work, we propose a processing pipeline for the calculation of the continuous velocity as well as the overall jump length. This computation is performed with a model-based jump phase segmentation, a correction for misalignment and an orientation determination of the skis at all times (see Fig. 1). Our complete pipeline is designed to process data from an unobtrusive measurement method with wearable sensors only attached to the skis, supported by data from a light barrier system at the take-off platform.

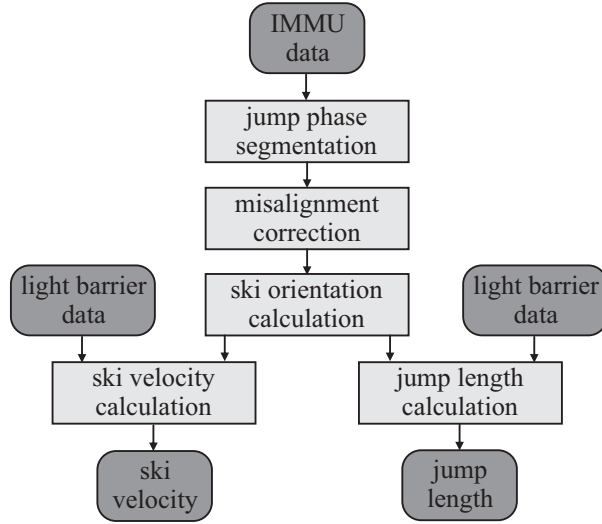


Fig. 1. Flowchart of complete processing pipeline from the IMMU and light barrier data to the ski velocity and jump length.

## 2 METHODS

### 2.1 Data acquisition

**2.1.1 Hardware.** The data acquisition was based on the *miPod* sensor system [6]. The sensor hardware contained an inertial-magnetic measurement unit with a three-axes accelerometer, a three-axes gyroscope and a three-axes magnetometer. The IMMU was configured to an accelerometer range of  $\pm 16$  g, a gyroscope range of  $\pm 2000$   $^{\circ}$ /s, a magnetometer range of  $\pm 1200$   $\mu$ T and a sampling rate of 200 Hz with a 16-bit resolution per axis.

In addition to the sensor hardware, a camera system was built up in order to be used for later evaluation. It consisted of four synchronized and simultaneously recording cameras. One camera covered the start area at the top of the jumping hill, one the take-off area and two cameras were used to record the landing. The cameras were set to a sampling rate of 100 Hz with their maximum resolution of 640 x 480 pixels. For the synchronization of the IMMU and the camera system, a method was developed based on the combination of a magnetic gate and a light barrier pair (response time:  $\pm 0.5$  ms) at the same position on the jumping hill, 6 m before the end of the take-off platform (see Fig. 2). The magnetic gate was created using four permanent magnets (two for the left ski, two for the right ski), which produced a magnetic field that was multiple times stronger than the earth magnetic field. When an athlete passed this setup, the IMMU magnetometer measurement showed a clear peak in the signal while the light barrier was triggered simultaneously. The light barrier and the camera system were connected to the same base station and therefore followed the same time. In addition, a second pair of light barriers was built up at the end of the take-off platform, that is, with a distance of 6 m to the first pair. The combination of both pairs was used for the establishment of the ground truth take-off velocity for evaluation purposes.

**2.1.2 Study design.** Inertial-magnetic sensor data were acquired during two ski jumping training sessions at the HS 106 *Fichtelbergschanze* [22] in Oberwiesenthal, Germany. One training session was conducted in summer season and one in winter season. In total, eleven experienced athletes (all male, average age [years]:  $16 \pm 1$ , jump experience [years]:  $10 \pm 2$ , height [cm]:  $176 \pm 9$ , weight [kg]:  $59 \pm 6$ ) of the Ski Association Saxony participated in the study. All athletes were aware of jump-related risks and the ski association gave written consent for the collected data to be published.



Fig. 2. Magnetic gate in combination with a light barrier system. IMMUs and global time were synchronized by evoking a distinct peak in the magnetometer signal while at the same time triggering the light barrier.

At the beginning of each session, the IMMUs were calibrated by performing a specified calibration procedure. The IMMU calibration was necessary to estimate current internal sensor parameters (e.g., measurement bias, scaling factors and cross-sensitivity) [17] and to provide accurate data for later processing. Besides the variation of these parameters over time, the change of the outside temperature influences the IMMU output [16, 33]. In order to avoid inaccuracies due to temperature differences (especially in winter season), the sensor hardware was acclimatized to the outside temperature before starting the calibration procedure. Subsequently, multiple sensors were attached to a calibration cube which was moved following a pre-defined motion pattern. This motion pattern contained static positions on all six sides of the cube as well as multiple rotations about all axes. A rotary table with adjustable stand was used to provide a stable calibration environment even on snow-covered ground. The whole calibration hardware is visualized in Fig. 3.

After the calibration procedure was performed, one sensor was attached to each ski with VELCRO® adhesive tape. The sensor orientation was defined by the sensor's x-axis representing the sagittal, the y-axis the frontal and the z-axis the longitudinal axis of the athlete (see Fig. 4). The training sessions were executed by the athletes without any specific consideration of the data acquisition being performed. No involvement of the athlete was necessary. One training session usually consisted of two to six consecutive jumps, depending on the athlete and training conditions. In total, data of 34 jumps were collected with two IMMUs per athlete. However, due to isolated incidents of device failure, 34 jumps of the right sensor but only 24 jumps of the left sensor could be stored for later evaluation. The missing data were the result of an early application of our recently developed sensor hardware. Although the sensing process itself is robust and reliable, the data storage is error-prone regarding power outages and unwary user interaction during the data download process. As a result, the data of two (left) sensors were deleted before or during downloading. In addition to the IMMU data, all jumps were recorded with the camera system and detailed field records were kept for all acquisitions.

**2.1.3 Sensor calibration.** The initial sensor calibration was based on the sensor measurements of six static positions and rotations about all axes. With these data, the accelerometer and the gyroscope were calibrated following an adapted version of the algorithm of Ferraris and colleagues [14]. They considered a gyroscope calibration with rotations of  $360^\circ$ . In our adapted version, multiple rotations about each axis were performed in order to minimize the influence of inaccurate rotation performance. The magnetometer was only used for the synchronization with the light barrier-triggered camera system. Hence, a calibration of the magnetometer was not required.

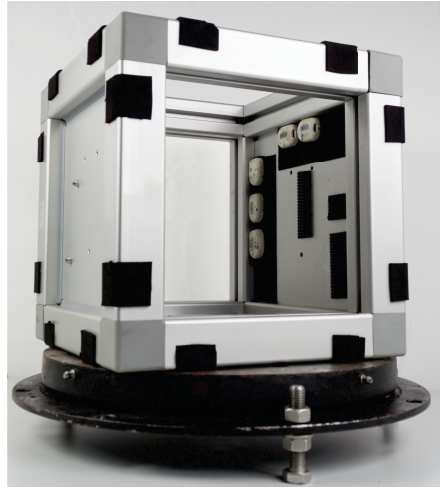


Fig. 3. Calibration cube for a stable calibration of multiple sensors. The cube was placed in six stable static positions on top of a rotary table and was rotated about all axes. The *miPod* IMMUs were attached to the inside of the cube.

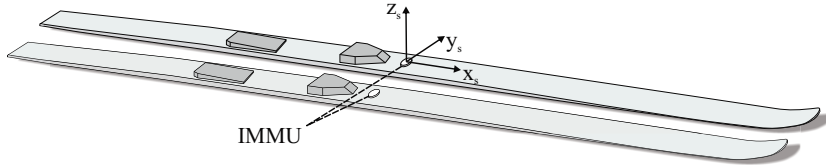


Fig. 4. Sensor attachment to both skis in front of the binding with corresponding sensor-ski coordinate system

**2.1.4 Definition of coordinate systems.** For the processing of the acquired data, two coordinate systems were defined: the ski system  $s$  and the global system  $g$  as shown in Fig. 5. If not otherwise stated, all vectors and matrices refer to the global coordinate system. Vectors  $\mathbf{v}$  that refer to the ski system are marked with  $\mathbf{v}^s$ . The rotation from the global to the ski system  $C_{g,t}^s$  equals the orientation of the ski in the global system  $C_{ski,t}$  at time  $t$ .

## 2.2 Phase segmentation

In order to prepare the obtained data for further processing, a segmentation of the jump was conducted. The whole jump scenario was separated in five phases: rest (non-motion state before the start), straight inrun, radius, take-off preparation and flight. In addition, the following points of time were defined: start motion, take-off and landing. An overview of the defined states and times is provided in Fig. 5.

In the literature, several algorithms were proposed that could be applied for the segmentation of each jump into the defined phase. Amongst them were template-based segmentations such as Subsequent Dynamic Time Warping [5, 31] with examples in gait analysis [3, 4] and rowing [19] as well as model-based approaches such as Hidden Markov Models (HMM) [34] with examples in gait segmentation [29], ECG signal segmentation [1] and swimming [13]. Considering possible extensions and adaptations of our system with future data recordings, a model-based approach would allow the possibility of learning more diverse data than a template-based approach.

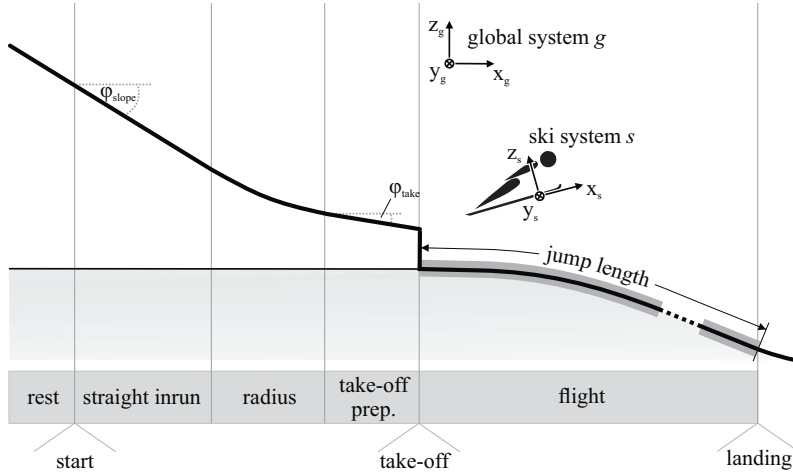


Fig. 5. Schematic representation of a jump scenario (not drawn to scale).

Hence, we decided to implement a Hidden Markov Model. Due to the hierarchical nature of our data, we specifically chose a Hierarchical Hidden Markov Model (HHMM) [15] for the application in ski jumping.

The top hierarchical level of our HHMM contained the five ski jump phases (see Fig. 5). Each of these five ski jump phases consisted of a further HMM containing  $N$  hidden states. The jump phases were trained fully supervised with ten iterations. In contrast, the hidden states of the lower hierarchy HMMs were trained unsupervised. All transitions were defined as forced left-to-right transitions as in [32]; that is, the model could not return to a state that it had previously left and only had the ability to move to the next available state in the sequence. Furthermore, they were implemented with forced alignment in order to ensure starting with the first state of the rest phase and ending with the last state of the flight phase. The suitable number of hidden states for the proposed pipeline  $N$  was analyzed in a previous study and defined to  $N = 3$ . We used a Gaussian Mixture Model (GMM) to model the continuous data input. This model was initialized with ten centers. The calculated features were the raw acceleration signals of x- and z-axes, the raw gyroscope signal of the y-axis, the cumulative sum of the gyroscope y-axis over the complete jump and the variances of all aforementioned features.

The ground truth labels for training the model and later evaluation were established by simultaneous analysis of the video and sensor data. Due to the fact that the only available training data were also needed to test the rest of the pipeline, a leave-one-subject-out training approach was used. Thus, eleven different hierarchical HMM were trained. This means that the model used to segment data for the rest of the pipeline was trained on the data for all skiers excluding the current one.

In contrast to related literature [12, 37], the proposed phase definition did not distinguish between different flight phases such as early flight and stable flight. However, this was not necessary for the calculation of the required parameters for the proposed pipeline. Instead, in our approach, we considered a more detailed segmentation of the inrun on the jumping hill (straight inrun, radius, take-off preparation). These phases were necessary for the misalignment correction which will be explained in detail in the following section.

### 2.3 Misalignment correction

For achieving the maximum accuracy of the calculated parameters, it was important that the sensor and the ski frame were aligned correctly. Hence, a correction of any misalignment caused by the placement of the sensor

on the ski was necessary. Due to the requirement of unobtrusiveness, the athlete's active participation in the measurement had to be avoided. Therefore, a functional calibration procedure was implemented following the approach of [20]. For the rotation from the sensor to the ski frame, measurements of two known states were incorporated: the rest phase before the start and the radius of the inrun.

The basic idea of the misalignment correction was to measure the gravity components per sensor axis in the rest phase  $\mathbf{a}_{meas,rest}^s$  and the rotation angle per sensor axis during the radius phase  $\theta_{meas,radius}^s$ , which was calculated by the integration of the gyroscope signal. In a perfectly aligned sensor-ski system, the measured gravity would exactly reflect the orientation of the ski in the rest phase and the rotation in the inrun radius would only be measured in the y-axis of the gyroscope (frontal axis of the athlete). However, due to possible misalignment, both vectors could vary from the expected vectors  $\mathbf{a}_{exp,rest}^s$  and  $\theta_{exp,radius}^s$ . Based on the two-stage approach of [20], the misalignment was computed and corrected for all obtained data sets.

## 2.4 Ski orientation

The initial ski orientation  $C_{ski,init}$  was known based on the slope angle  $\varphi_{slope}$  at the starting position (in this work:  $\varphi_{slope} = 37.0^\circ$ ) [22]. All further rotations of the ski were measured by the gyroscope. The gyroscope signal was integrated with the quaternion-based approach as described in [20]. The resulting quaternion  $\mathbf{q}_{t0}^{t1}$  contained the rotation of the ski system from time  $t0$  to time  $t1$ . Based on the initial ski orientation  $C_{ski,init}$ , the ski orientation  $C_{ski,t}$  at all times  $t$  was calculated with a quaternion multiplication [27].

$$C_{ski,t} = \mathbf{q}_{init}^t \cdot C_{ski,init} \quad (1)$$

However, due to sensor noise during the inrun phase, it was more accurate to reset the integration of the gyroscope at the additionally known state before the take-off instant. There, the skis are still in the track and hence, the ski orientation equals the orientation of the take-off platform. The orientation  $C_{ski,take}$  can be obtained by incorporating the take-off platform pitch angle  $\varphi_{take}$  (in this work:  $\varphi_{take} = 10.5^\circ$ ). Hence, the ski orientation  $C_{ski,t}$  was calculated based on the initial ski orientation until the take-off and based on the take-off orientation for the flight phase.

$$C_{ski,t} = \begin{cases} \mathbf{q}_{init}^t \cdot C_{ski,init} & \text{for } t \in [t_{init}, t_{take}] \\ \mathbf{q}_{take}^t \cdot C_{ski,take} & \text{for } t \in [t_{take}, t_{land}] \end{cases} \quad (2)$$

## 2.5 Ski velocity

The ski velocity calculation was performed by integrating the accelerometer measurements as proposed for applications of strapdown inertial navigation in [35]. However, the influence of gravity had to be considered and eliminated. Therefore, the gravity vector  $\mathbf{a}_{grav} = [0, 0, g]^\top$  was transformed into the ski coordinate system at each time step  $t$ .

$$\mathbf{a}_{grav,t}^s = C_{ski,t} \cdot \mathbf{a}_{grav} \quad (3)$$

Subsequently,  $\mathbf{a}_{grav,t}^s$  was subtracted from all corresponding acceleration measurements. The resulting acceleration vector  $\mathbf{a}_{motion,t}^s$  was assumed to contain only the actual motion acceleration at each time step  $t$ . The corresponding velocity  $\mathbf{v}_{motion,t}^s$  could then be calculated by integration of  $\mathbf{a}_{motion,t}^s$  over  $t$  considering a possible prior velocity  $\mathbf{v}_0^s$ . For discrete measurements, the integral can be approximated by

$$\mathbf{v}_{motion,t}^s = \mathbf{v}_0^s + \sum \mathbf{a}_{motion,t}^s \cdot \Delta t. \quad (4)$$

The overall ski velocity  $v_t^s$  was computed by the norm of the resulting velocity vector.

$$v_t^s = \|\mathbf{v}_{motion,t}^s\|_2 \quad (5)$$

The calculation was performed separately for the two time intervals [start to take-off] and [take-off to landing]. This was necessary for two reasons: the influence of vibrations during accelerating on the slope and an improvement of accuracy by a velocity update based on the light barrier system at the take-off.

**2.5.1 Ski velocity from start to take-off.** In the first time interval, the athletes accelerated on the slope. Due to contact with the slope and an uneven surface, the acceleration measurement was influenced by vibrations of the skis. In order to minimize this influence, prior knowledge of the motion direction was incorporated. During the inrun, the only relevant motion acceleration was measured in the x-direction of the ski system. Hence, measurements of the y- and z-axes were ignored for the ski velocity determination. In addition, the prior velocity  $\mathbf{v}_0^s$  was set to zero due to the rest state before the start of the motion. The resulting continuous velocity before the take-off was then calculated by adapting (4) to (6).

$$\mathbf{v}_{motion,t}^s = \sum \begin{pmatrix} a_{x,motion,t}^s \\ 0 \\ 0 \end{pmatrix} \cdot \Delta t \quad \text{for } t \in [t_{init}, t_{take}] \quad (6)$$

**2.5.2 Ski velocity from take-off to landing.** During the flight phase, there was no influence caused by vibrations and, in addition, the skis' acceleration was no longer restricted to the y-axis. Therefore, all components of the motion acceleration vector  $\mathbf{a}_{motion,t}^s$  were used for the velocity calculation. Instead of basing the flight velocity on the possibly erroneous acceleration integration of the first interval, the take-off velocity was updated with the light barrier system at the take-off platform. Hence, the prior velocity  $\mathbf{v}_0^s$  was set to the light barrier velocity  $v_{lb}$ . Based on the defined movement of the skis before the take-off, the velocity measured by the light barrier completely represented the ski's velocity in x-direction. The resulting continuous velocity for the flight phase was calculated by

$$\mathbf{v}_{motion,t}^s = \begin{pmatrix} v_{lb} \\ 0 \\ 0 \end{pmatrix} + \sum \mathbf{a}_{motion,t}^s \cdot \Delta t \quad \text{for } t \in [t_{take}, t_{land}]. \quad (7)$$

## 2.6 Jump length

The jump length calculation was based on the previously established parameters of motion acceleration, ski orientation and velocity as well as the instants of take-off and landing. The current position of the sensor  $\mathbf{x}_t$  in the global system at time  $t$  could then be computed by applying the motion model of accelerated movements.

$$\mathbf{x}_t = \mathbf{x}_{t-1} + C_{ski,t}^{-1} \cdot \left[ \mathbf{v}_{motion,t-1}^s \cdot \Delta t + \frac{1}{2} \cdot \mathbf{a}_{motion,t}^s \cdot \Delta t^2 \right] \quad (8)$$

For the determination of the actual jump length  $w$  as it is defined by the *Standards for the Construction of Jumping Hills* [21], a further ramp-specific transformation was necessary. Referring to [21], the jump length is defined by the ground distance from the end of the take-off platform to the landing position (see Fig. 5). In order to transform the landing position  $\mathbf{x}_{t=t_{land}}$  from the global system to the official jump length, a mathematical model of the jumping hill was established with the parameters of the *Jumping Hill Certificate* [22]. Based on this model, the horizontal component of  $\mathbf{x}$  was processed to the jumping hill-specific jump length  $w$  with the following procedure.

The landing slope of a jumping hill is defined for specific points P, K, and L. The jump lengths  $w(P)$ ,  $w(K)$  and  $w(L)$  were known based on the hill certificate. Furthermore, the horizontal component  $x$  of  $\mathbf{x}$  was known for

these points based on the equations of [21]:

$$\begin{aligned} x(P) &= n - r_L \cdot (\sin\beta_P - \sin\beta) \\ x(K) &= n \\ x(L) &= n + r_L \cdot (\sin\beta - \sin\beta_L), \end{aligned} \tag{9}$$

with the jumping hill specific parameters  $n$ ,  $r_L$ ,  $\beta$ ,  $\beta_P$ ,  $\beta_L$ . The corresponding jump length  $w$  for each jump of this work was then computed based on a linear interpolation between the known horizontal distance and jump length pairs.

## 2.7 Evaluation

**2.7.1 Ground truth measurements and data sets.** Two external systems were incorporated for the evaluation: the light barriers for the velocity measurement at the take-off platform as well as the camera system for the jump phase segmentation and the jump length analysis. Based on the light barrier response time of  $\pm 0.5$  ms and an estimated average velocity at the take-off of  $25.0 \frac{\text{m}}{\text{s}}$ , the accuracy of the light barrier system was calculated to be  $\pm 0.10 \frac{\text{m}}{\text{s}}$ . The accuracy of the video camera system was relevant for the phase segmentation and jump length evaluation. The camera frames were analyzed manually with *Kinovea* video software [25]. For the evaluation of the jump length, the landing frame was overlaid by a measurement grid to simplify the ground truth determination (see Fig. 6). Due to the frame rate of 100 Hz and the estimated average velocity of  $25.0 \frac{\text{m}}{\text{s}}$ , the accuracy of the system was restricted to  $\pm 0.25$  m. However, the accuracy was assumed to be worse than this value based on the limited quality of the camera recording. Experimentally, the uncertainty of the annotation was found to be up to three frames. This equals a distance of up to  $\pm 0.75$  m.

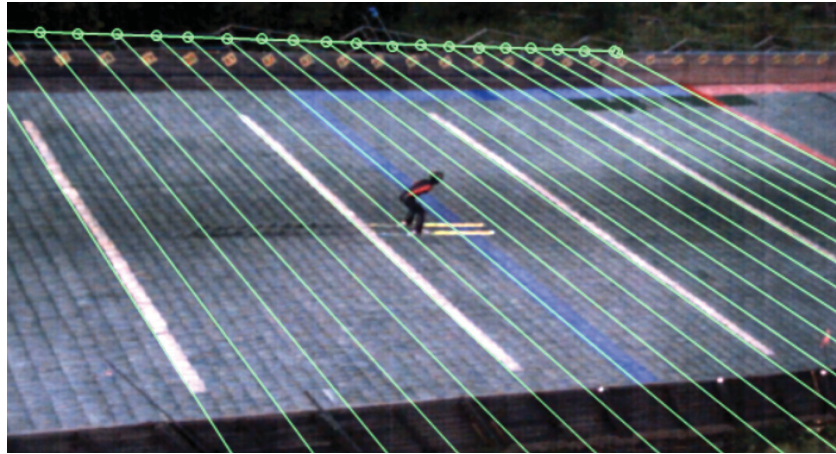


Fig. 6. Manual jump length analysis with the camera system and *Kinovea* video software.

The evaluation of the phase segmentation, the ski velocity and the jump length were based on all 58 available data sets without differentiation between left and right. Only the relative comparison of the velocity required a combined analysis of both skis. Hence, the 24 complete data sets were used for that purpose. An overview of the evaluation contents with corresponding data sets is provided in Table 1. Details of the evaluation procedure are given in the following sections.

Table 1. Overview of evaluation procedure, corresponding data sets and the error with respect to ground truth (absolute) / difference between left and right ski (relative).

content	procedure	data sets	error / difference
phase segmentation	validation of HHMM-segmented jump phases against video labeled data	24 left, 34 right	see Tab. 2
ski velocity (absolute)	validation against ground truth data of light barrier system at take-off platform	24 left, 34 right	$-0.78 \frac{m}{s} \pm 1.18 \frac{m}{s}$ ( $-3.0\% \pm 4.7\%$ )
ski velocity (relative)	comparison of left and right ski sensor during flight phase	24 combined	$0.40 \frac{m}{s} \pm 0.96 \frac{m}{s}$
jump length	validation against ground truth data of camera system at landing instant	24 left, 34 right	$0.8 \text{ m} \pm 2.9 \text{ m}$ ( $0.9\% \pm 3.4\%$ )

2.7.2 *Phase segmentation evaluation.* The HHMM-based segmentation accuracy was compared to the video labeled ground truth. The most crucial state transitions for the calculation of jump parameters were the start of the motion, take-off and landing. Although the other defined transitions were also part of the pipeline, their accuracy was not as relevant as the aforementioned ones. In addition, there was no video labeled ground truth data available for these transitions and the model was trained based on a manual signal analysis. Therefore, the evaluation was limited to the three transitions: start of the motion, take-off and landing. The error was calculated by the mean and standard deviation of  $(t_{phase,HHMM} - t_{phase,gt})$ .

2.7.3 *Ski velocity evaluation.* The velocity calculation of each ski was validated with reference to the ground truth measurement at the take-off platform. Thus,  $v_t^s$  was compared to the light barrier system measurement  $v_{lb}$  at the take-off by  $(v_t^s - v_{lb})$  for  $t = t_{take}$ . For the evaluation, the mean and standard deviation of the velocity error were calculated over all jumps. In addition, the error was calculated in percentage of the estimated average take-off velocity of  $25.0 \frac{\text{m}}{\text{s}}$ .

Furthermore, a continuous velocity evaluation for the flight phase was performed by a relative comparison of left and right ski. The velocity development was analyzed over all jumps by the mean and standard deviation of  $(v_{t, left}^s - v_{t, right}^s)$ .

2.7.4 *Jump length evaluation.* For the evaluation of the jump length  $w$ , the calculated value was compared to the manually determined ground truth jump length  $w_{gt}$  by  $(w - w_{gt})$ . The mean and standard deviation of the error to ground truth data were determined over all jumps. In addition, the error was calculated as a percentage of the average jump length over all jumps (average jump length in our acquisition: 84.5 m).

### 3 RESULTS

#### 3.1 Phase segmentation results

The deviation of the proposed phase segmentation to the ground truth data is provided in Tab. 2.

#### 3.2 Ski velocity results

For the absolute ski velocity evaluation, the computed velocity was compared to the light barrier ground truth. The mean and standard deviation of the error were determined to be  $-0.78 \frac{\text{m}}{\text{s}} \pm 1.18 \frac{\text{m}}{\text{s}}$ . This equals a percentage

Table 2. Results: Error of HHMM-based jump phase segmentation compared to the video labeled ground truth by  $(t_{phase,HHMM} - t_{phase,gt})$

	start of motion	take-off	landing
mean [s]	0.01	-0.01	0.00
std. dev. [s]	0.83	0.08	0.05

of  $-3.0\% \pm 4.7\%$  in reference to the estimated average take-off velocity. The difference of the relative velocity calculation for left and right ski are provided in Fig. 7. Averaged over the complete flight phase, the difference was calculated to be  $0.40 \frac{m}{s} \pm 0.96 \frac{m}{s}$ .

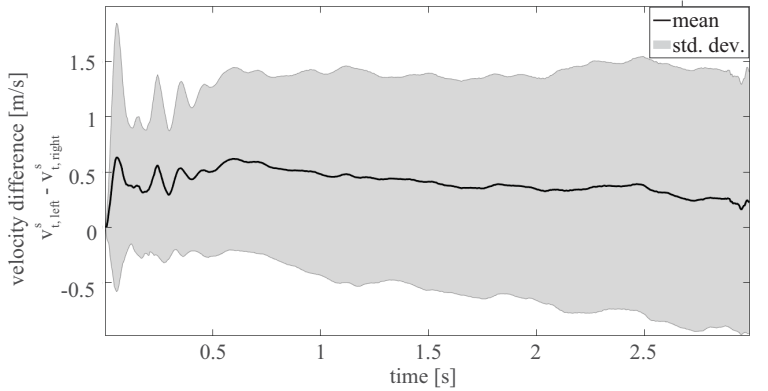


Fig. 7. Results: Comparison of the velocity development of left and right ski averaged over all evaluated jumps. The visualization starts at the take-off and ends with the landing instant of the jump with the shortest jump duration.

### 3.3 Jump length results

For the jump length evaluation, the mean and standard deviation of the error compared to the video-based ground truth were determined to be  $0.8 \text{ m} \pm 2.9 \text{ m}$ . This error can be interpreted as  $0.9\% \pm 3.4\%$  with reference to the average jump length.

## 4 DISCUSSION

### 4.1 Interpretation of results

The Hierarchical HMM-based segmentation showed sufficiently accurate results for the performance of the complete processing pipeline. Although the mean values of the errors compared to the video-based system are within the sampling accuracy of the hardware components (sensor: 200 Hz, cameras: 100 Hz), the standard deviation of the results was considerably high for the start of the motion. One reason for this is based on the physical differences of the initial motion sequence of each athlete. Whereas some athletes start with their skis already resting in the track, others move their skis back and forth multiple times and then directly jump into the track for initiating the movement. These motion differences could be considered by including data of more than eleven athletes as in the case of this work. A large number of data sets of various athletes would lead to a better incorporation of individual jump techniques in the training of the model and hence, would possibly lead to a more robust segmentation performance.

For the velocity calculation at the take-off, the results show an error compared to the light barrier system of  $-0.78 \frac{m}{s} \pm 1.18 \frac{m}{s}$  and a relative difference between left and right of  $0.40 \frac{m}{s} \pm 0.96 \frac{m}{s}$ . This reflects a consistent processing of measurements on the inrun slope as well as in the flight phase. Considering an average velocity of  $25.0 \frac{m}{s}$ , the calculated error is in a range of under 5 %. Although such an error would probably not be acceptable for quantitative judgments in competitions, it could be used as a visualization tool for spectators or for the analysis during training sessions. In addition, the jump velocity could further be analyzed in horizontal and vertical components and thus show the velocity and possibly also the forces applied at the landing impact. Analyzing the continuous velocity development could furthermore provide interesting feedback for coaches and athletes who could compare to their previous jumps and to those of others.

For the jump length calculation, the error was calculated to be  $0.8 \text{ m} \pm 2.9 \text{ m}$ , which is  $0.9\% \pm 3.4\%$  of the average jump length of this work. These numbers can be interpreted similarly to the velocity evaluation. Compared to a standardized camera-based jump length measurement with an accuracy of  $\pm 0.5 \text{ m}$  [23], the proposed system cannot be used for judging in competitions. However, it could support competitions. While a camera-based analysis only covers the landing position, a sensor-based method monitors the whole flight phase. Thus, not only the jump length but also the flight path could be provided. This would lead to a new way of attractive visualization for spectators, e.g., by showing the influence of gusts. However, the evaluation of the flight path was not in the scope of this work and remains to be established in future work. Still, due to the results of the jump length, the flight path can be assumed to be in a certain accuracy and the proposed system could already be used in training sessions as an indicator of the performance and skills of an athlete. Possible applications for training support could include a visualization of the flying altitude in dependency of the covered distance or an analysis of the altitude compared to the horizontal and vertical velocity. Based on this information, also the flight style can be analyzed in detail by distinguishing between rather flat but fast and rather high but slow flight performances. In addition, the in- and decrease of velocity could be monitored during inrun, take-off, flight phase and landing preparation. The latter can be analyzed by incorporating the landing angle in combination with the velocity components.

For scientific purposes, the required accuracy of the velocity estimation was established to be  $\pm 0.1 \frac{km}{h}$  for the inrun [26] and can be assumed to be about  $\pm 0.5 \frac{km}{h}$  for the flight phase. However, for practical application, the accuracy requirements are more relaxed and the output provided by the proposed system can be assumed to be helpful for coaches considering that currently there is no other inexpensive system for measuring the continuous velocity development. Furthermore, the velocity development itself contains more relevant information than the actual absolute velocity for most analyses. A similar situation can be found for flight path analyses. For coaches, the development between velocity and altitude is usually more interesting than an absolute value of the altitude.

## 4.2 Influencing aspects and improvements

For the discussion of possible accuracy improvements, two major aspects should be considered: the influence of the processing steps before calculating the proposed parameters and the accuracy of the ground truth system. The processing chain leading to the velocity and jump length calculation includes the misalignment, the phase segmentation and the orientation determination (see Fig. 1). Although the fundamentals of the applied methods have been evaluated or published in previous work, they have not been completely validated for absolute accuracy. The misalignment was proposed in the complete processing pipeline of [20] but only the final results were evaluated. The previous work on Hierarchical HMM was modified to a phase segmentation in ski jumping. Although the most relevant state transitions were evaluated in this work, a complete analysis with more data and ground truth for all transitions would possibly enhance the segmentation accuracy. The ski orientation was investigated in several publications [9, 10, 20], however only evaluated with a comparison to literature values or with analysis of single angles rather than a complete 3D-orientation over the whole flight phase. Hence, this work

proposes a working processing pipeline with evaluated final results, but the overall accuracy could be improved by including extended analyses of all individual components.

The second aspect influencing the final results is the ground truth. Both the light barrier as well as the camera-based jump length measurements could introduce inaccuracies to the evaluation. The light barriers were installed in a way that they were triggered by the bindings of the skis (see Fig. 2) and not by the body of the athlete which would lead to deviations in the measurements due to a considerably varying body pose in the last part of the inrun. However, this procedure was not analyzed for accuracy. In addition, the jump length evaluation with the camera system covering the landing area could contain inaccuracies. These inaccuracies are a result of the limited resolution, the camera perspective and possible uncertainties in the manual labeling process. As stated before, an uncertainty of up to three frames should be considered. Further inaccuracies could be introduced based on the established model for the transformation from the landing position in the global system to the jump length  $w$ . Especially in winter, the influence of the snow layer on the slope should be measured and incorporated accurately. An improvement of the ground truth measurements could be a validated velocity determination and a camera system with higher resolution. In addition, a 3D-motion capture system with markers attached to both ends of the ski could provide the required ground truth of velocity, jump length and even the continuous flight path.

#### 4.3 Application in competitions and standard training

The design of the proposed system was established in consideration of previously stated requirements. In order to apply a jump analysis system to competitions and standard training, it must be unobtrusive, automated and affordable. With the proposed system, these goals were achieved. The sensor data were obtained from IMMUs at the skis and the light barrier system at the take-off platform. The sensors can be attached before the athlete prepares for the jump and the light barriers can easily be set up or are often already available at jumping hills. Although our system requires manual assistance for charging, calibrating and attaching the IMMU and light barrier hardware, the sensing and calculation itself does not require any interaction during the competition. The athletes who participated in our study reported no impairment by the wearable sensors. Furthermore, our results show that the collected data are sufficient for all required computations. With our algorithm, all processing steps can be performed without the necessity of experienced personnel or complex equipment. In addition, wearable sensors and light barriers are considerably cheaper than a camera-based system covering the landing area or even the complete jump scenario. However, it should be discussed that the proposed system requires certain adaptation according to the environment.

One aspect which should be considered in future studies is the influence of the temperature on the measurements. In our acquisitions, the sensors were calibrated at the beginning of each day and it was assumed that the temperature would not change significantly during the training session. In contrast, there are training sessions or even competitions that include drastic temperature changes and the sensors have to compensate for that [16, 33]. One method to establish a more robust system would be a calibration procedure that is scalable according to temperature. The basic calibration parameters such as measurement bias, scaling factors and cross-sensitivity do not change rapidly as long as there is a stable temperature. A temperature-compensating calibration could be trained automatically in order to adapt to the relevant parameters according to the current temperature.

Another aspect is the jumping hill size. While our study was conducted on a jumping hill size HS 106, competitions are usually performed on slightly larger jumping hills as e.g., HS 134 in [36]. The major impact would probably be seen in the HHMM-based segmentation which was trained on data of this study only. However, due to the nature of an advanced pattern recognition method, it can be assumed that the proposed segmentation can easily be adapted by adding training jumps of other jumping hills to the existing data sets. Due to varying slope structures, it must be assumed that a training phase is always necessary for incorporating new venues. Whereas some structural parameters may remain identical (e.g., landing platform inclination), there could be

variations in the landing slope inclination (given by P, K and L) or even in the thickness of the snow layer covering the slope. Aside from the segmentation part of our algorithm, the rest of the pipeline is based on physical motion models which should not be influenced by varying hill size.

Although the proposed pipeline has the capacity for a real-time application and can provide relevant information even for competitions, further extensions are required for an application in real-time. The described system and its evaluation were based on data that were stored on the sensor unit. For the application in real-time, a wireless transmission over the full distance of the jump area is necessary. Furthermore, the acquisition should be triggered automatically so that the processing starts when the athlete is in the start area and ends when the athlete finishes the landing. In addition, the measurement hardware has to be improved to avoid data loss which for instance occurred during the data acquisition of this work. Finally, an analysis of the community perception, similar to the one performed in [18], would assess the sports community's acceptance towards a wearable real-time system.

## 5 CONCLUSION AND FUTURE WORK

The goal of this work was the design of an unobtrusive, automated and affordable system that provides continuous ski velocity and jump length. We proposed a processing pipeline which was based on inertial-magnetic sensor data and light barrier measurements. The processing pipeline contained an automated jump phase segmentation and misalignment correction which ensured an automated computation without the requirement of any interaction from the athlete. The results showed that our system is capable of providing the ski velocity with an error of  $-0.78 \frac{m}{s} \pm 1.18 \frac{m}{s}$  and the jump length with an error of  $0.8 \text{ m} \pm 2.9 \text{ m}$ .

Aiming towards an application of our algorithm in competitions and standard training, a real-time system could be established. Therefore, further hardware developments are necessary. The next steps towards a real-time system are the establishment of a wide range data transmission and remotely controllable sensor hardware. While these developments still have to be achieved, an offline training support by our system is already achievable. The relevant parameters for training support, such as the ski orientation, velocity and jump length, are calculated in our pipeline. Hence, our system can be incorporated into the training process by storing obtained jump data and corresponding parameters for later comparison and analysis.

## ACKNOWLEDGMENTS

The authors thank the Ski Association Saxony (Skiverband Sachsen), especially coach Peter Grundig as well as all participants of the study for their support during the data collection. Bjoern Eskofier gratefully acknowledges the support of the German Research Foundation (DFG) within the framework of the Heisenberg professorship programme (grant number ES 434/8-1).

## REFERENCES

- [1] Rodrigo Varejão Andreão, Bernadette Dorizzi, and Jérôme Boudy. 2006. ECG signal analysis through hidden Markov models. *IEEE Transactions on Biomedical engineering* 53, 8 (2006), 1541–1549.
- [2] Marc Bächlin, Martin Kusserow, Gerhard Tröster, and Hanspeter Gubelmann. 2010. Ski jump analysis of an Olympic champion with wearable acceleration sensors. In *14th Int. Symp. on Wearable Computers*. 1–2.
- [3] Jens Barth, Cäcilia Oberndorfer, Patrick Kugler, Dominik Schuldhaus, Jürgen Winkler, Jochen Klucken, and Bjoern Eskofier. 2013. Subsequence dynamic time warping as a method for robust step segmentation using gyroscope signals of daily life activities. In *35th Annu. Int. Conf. of the IEEE Engineering in Medicine and Biology Society (EMBC)*. 6744–6747.
- [4] Jens Barth, Cäcilia Oberndorfer, Cristian Pasluosta, Samuel Schülein, Heiko Gassner, Samuel Reinfelder, Patrick Kugler, Dominik Schuldhaus, Jürgen Winkler, Jochen Klucken, and Bjoern M Eskofier. 2015. Stride segmentation during free walk movements using multi-dimensional subsequence dynamic time warping on inertial sensor data. *Sensors* 15, 3 (2015), 6419–6440.
- [5] Donald J Berndt and James Clifford. 1994. Using dynamic time warping to find patterns in time series. In *KDD workshop*. 359–370.
- [6] Peter Blank, Patrick Kugler, Heiko Schlarb, and Bjoern Eskofier. 2014. A Wearable sensor system for sports and fitness applications. In *19th Annu. Congr. of the European College of Sport Science*.
- [7] Heike Brock and Yuji Ohgi. 2016. Development of an inertial motion capture system for kinematic analysis of ski jumping. *Proc IMechE Part P: J Sports Engineering and Technology* (2016), 1–12.
- [8] Heike Brock, Yuji Ohgi, and Kazuya Seo. 2016. Development of an automated motion evaluation system from wearable sensor devices for ski jumping. *Procedia Engineering* 147 (2016), 694–699.
- [9] Julien Chardonnens, Julien Favre, Florian Cuendet, Gérald Gremion, and Kamiar Aminian. 2010. Analysis of stable flight in ski jumping based on parameters measured with a wearable system. In *28th Int. Symp. on Biomechanics in Sports*. 273–276.
- [10] Julien Chardonnens, Julien Favre, Florian Cuendet, Gérald Gremion, and Kamiar Aminian. 2013. A system to measure the kinematics during the entire ski jump sequence using inertial sensors. *J. of Biomechanics* 46, 1 (2013), 56–62.
- [11] Julien Chardonnens, Julien Favre, Florian Cuendet, Gérald Gremion, and Kamiar Aminian. 2014. Measurement of the dynamics in ski jumping using a wearable inertial sensor-based system. *J. of Sports Sciences* 32, 6 (2014), 591–600.
- [12] Julien Chardonnens, Julien Favre, Benoit Le Callennec, Florian Cuendet, Gérald Gremion, and Kamiar Aminian. 2012. Automatic measurement of key ski jumping phases and temporal events with a wearable system. *J. of Sports Sciences* 30, 1 (2012), 53–61.
- [13] Farzin Dadashi, Arash Arami, Florent Crettenand, Gregoire P Millet, John Komar, Ludovic Seifert, and Kamiar Aminian. 2013. A hidden Markov model of the breaststroke swimming temporal phases using wearable inertial measurement units. In *13th Int. Conf. on Body Sensor Networks (BSN)*. 1–6.
- [14] Franco Ferraris, Ugo Grimaldi, and Marco Parvis. 1995. Procedure for effortless in-field calibration of three-axial rate gyro and accelerometers. *Sensors and Materials* 7, 5 (1995), 311–330.
- [15] Shai Fine, Yoram Singer, and Naftali Tishby. 1998. The hierarchical hidden Markov model: analysis and applications. *Machine learning* 32, 1 (1998), 41–62.
- [16] Rita Fontanella, Domenico Accardo, Egidio Caricati, Stefano Cimmino, Domenico De Simone, and Giovanni Lucignano. 2017. Improving inertial attitude measurement performance by exploiting MEMS gyros and neural thermal calibration. In *AIAA Information Systems-AIAA Infotech@ Aerospace*. AIAA, 1–8.
- [17] Mark Gaffney, Michael Walsh, Brendan O’Flynn, and Cian Ó Mathúna. 2011. An automated calibration tool for high performance wireless inertial measurement in professional sports. In *IEEE Sensors*. 262–265.
- [18] Benjamin H Groh, Jasmin Flaschka, Markus Wirth, Thomas Kautz, Martin Fleckenstein, and Bjoern M Eskofier. 2016. Wearable real-time skateboard trick visualization and its community perception. *IEEE Computer Graphics and Applications* 36, 5 (2016), 12–18.
- [19] Benjamin H Groh, Samuel J Reinfelder, Markus N Streicher, Adib Taraben, and Bjoern M Eskofier. 2014. Movement prediction in rowing using a dynamic time warping based stroke detection. In *9th Int. Conf. on Intelligent Sensors, Sensor Networks and Information Processing (ISSNIP)*. 1–6.
- [20] Benjamin H Groh, Nicolas Weeger, Frank Warschun, and Bjoern M Eskofier. 2014. Simplified orientation determination in ski jumping using inertial sensor data. In *DGON Inertial Sensors and Systems Symp. (ISS)*. 1–11.
- [21] International Ski Federation 2012. Standards for the construction of jumping hills. (2012).
- [22] International Ski Federation 2014. Certificate of jumping hill, no. 58 / GER 47, Oberwiesenthal. (2014).
- [23] International Ski Federation 2015. The International ski competition rules (ICR). (2015).
- [24] Alexander Jung, Manfred Staat, and Wolfram Müller. 2014. Flight style optimization in ski jumping on normal, large, and ski flying hills. *J. of Biomechanics* 47, 3 (2014), 716–722.
- [25] Kinovea, 2016 accessed: February 01, 2017. Open source video analysis software. (accessed: February 01, 2017). [Online.] <http://www.kinovea.org>.
- [26] Sascha Kreibich, Sören Müller, Mario Kürschner, and Ilka Seidel. 2017. Leistungsfaktor Anfahrtsgeschwindigkeit. *Leistungssport* 1 (2017), 31–35.

- [27] Jack B Kuipers. 1999. Quaternions and rotation sequences. In *1st Int. Conf. on Geometry, Integrability and Quantization*. 2127–143.
- [28] Grega Logar and Marko Munih. 2015. Estimation of joint forces and moments for the in-run and take-off in ski jumping based on measurements with wearable inertial sensors. *Sensors* 15, 5 (2015), 11258–11276.
- [29] Andrea Mannini, Diana Trojaniello, Ugo Della Croce, and Angelo M Sabatini. 2015. Hidden Markov model-based strategy for gait segmentation using inertial sensors: Application to elderly, hemiparetic patients and Huntington’s disease patients. In *37th Annu. Int. Conf. of the IEEE Engineering in Medicine and Biology Society (EMBC)*. 5179–5182.
- [30] Erich Müller and Hermann Schwameder. 2003. Biomechanical aspects of new techniques in alpine skiing and ski-jumping. *J. of Sports Sciences* 21, 9 (2003), 679–692.
- [31] Meinard Müller. 2007. Dynamic time warping. In *Information retrieval for music and motion*. Springer, Chapter 4, 69–84.
- [32] Ghazaleh Panahandeh, Nasser Mohammadiha, Arne Leijon, and Peter Händel. 2013. Continuous hidden Markov model for pedestrian activity classification and gait analysis. *IEEE Transactions on Instrumentation and Measurement* 62, 5 (2013), 1073–1083.
- [33] Igor P Prikhodko, Alexander A Trusov, and Andrei M Shkel. 2013. Compensation of drifts in high-Q MEMS gyroscopes using temperature self-sensing. *Sensors and Actuators A: Physical* 201 (2013), 517–524.
- [34] Lawrence R Rabiner. 1989. A tutorial on hidden Markov models and selected applications in speech recognition. *Proc. IEEE* 77, 2 (1989), 257–286.
- [35] Paul G Savage. 1998. Strapdown inertial navigation integration algorithm design part 2: velocity and position algorithms. *J. of Guidance, Control, and Dynamics* 21, 2 (1998), 208–221.
- [36] Bernhard Schmölzer and Wolfram Müller. 2005. Individual flight styles in ski jumping: results obtained during Olympic Games competitions. *J. of Biomechanics* 38, 5 (2005), 1055–1065.
- [37] Hermann Schwameder. 2008. Biomechanics research in ski jumping, 1991–2006. *Sports Biomechanics* 7, 1 (2008), 114–136.
- [38] Mikko Virmavirta, Juha Isolehto, Paavo Komi, Hermann Schwameder, Fabio Pigozzi, and Giuseppe Massazza. 2009. Take-off analysis of the Olympic ski jumping competition (HS-106m). *J. of Biomechanics* 42, 8 (2009), 1095–1101.
- [39] Janez Vodičar, Milan Čoh, and Bojan Jošt. 2012. Kinematic structure at the early flight position in ski jumping. *J. of Human Kinetics* 35, 1 (2012), 35–45.

Received February 2017; accepted July 2017